β-delayed γ decay of ^{20}Mg and the ^{19}Ne(p, γ)^{20}Na breakout reaction in Type I X-ray bursts

B.E. Glassman [a,b,*], D. Pérez-Loureiro [b,*], C. Wrede [a,b,*], J. Allen [c], D.W. Bardayan [c], M.B. Bennett [a,b], B.A. Brown [a,b], K.A. Chipps [d,e], M. Febbraro [d,e], M. Friedman [b], C. Fry [a,b], M.R. Hall [c], O. Hall [c], S.N. Liddick [b,f], P. O'Malley [c], W.J. Ong [a,b], S.D. Pain [d], C. Prokop [b,f], S.B. Schwartz [a,b], P. Shidling [g], H. Sims [h], P. Thompson [d,e], H. Zhang [a,b]

[a] Department of Physics and Astronomy, Michigan State University, East Lansing, MI 48824, USA
[b] National Superconducting Cyclotron Laboratory, Michigan State University, East Lansing, MI 48824, USA
[c] Department of Physics, University of Notre Dame, Notre Dame, IN 46556, USA
[d] Oak Ridge National Laboratory, Oak Ridge, TN 37831, USA
[e] Department of Physics and Astronomy, University of Tennessee, Knoxville, TN 37996, USA
[f] Department of Chemistry, Michigan State University, East Lansing, MI 48824, USA
[g] Cyclotron Institute, Texas A & M University College Station, TX 77843, USA
[h] University of Surrey, GU2 7XH, Guildford, UK

ARTICLE INFO

ABSTRACT

Certain astrophysical environments such as thermonuclear outbursts on accreting neutron stars (Type-I X-ray bursts) are hot enough to allow for breakout from the Hot CNO hydrogen burning cycles to the rapid proton capture (rp) process. An important breakout reaction sequence is ^{15}O$(α,γ)^{19}$Ne$(p,γ)^{20}$Na and the ^{19}Ne$(p,γ)^{20}$Na reaction rate is expected to be dominated by a single resonance at 457 keV above the proton threshold in ^{20}Na. The resonance strength and, hence, reaction rate depends strongly on whether this ^{20}Na state at an excitation energy of 2647 keV has spin and parity of 1^+ or 3^+. Previous ^{20}Mg ($J^π = 0^+$) $β^+$ decay experiments have relied almost entirely on searches for $β$-delayed proton emission from this resonance in ^{20}Na to limit the log ft value and, hence, $J^π$. However there is a non-negligible $γ$-ray branch expected that must also be limited experimentally to determine the log ft value and constrain $J^π$. We have measured the $β$-delayed $γ$ decay of ^{20}Mg to complement previous $β$-delayed proton decay work and provide the first complete limit based on all energetically allowed decay channels through the 2647 keV state. Our limit confirms that a 1^+ assignment for this state is highly unlikely.

© 2018 The Authors. Published by Elsevier B.V. This is an open access article under the CC BY license (http://creativecommons.org/licenses/by/4.0/). Funded by SCOAP³.

1. Introduction

Type I X-ray bursts can be observed in the galaxy using space-based telescopes. The likely sites of these periodic sources are on the surfaces of neutron stars that accrete matter from hydrogen-rich binary partners [1,2]. The accreted material becomes so hot and dense that thermonuclear runaway occurs causing the X-ray luminosity of the system to spike suddenly and then relax on timescales of seconds to minutes. In type-I X-ray bursts new chemical elements are thought to be created by the rapid proton capture (rp) process [3], which involves a series of proton captures and $β^+$

decays up to $A \simeq 100$ [1]. Most of the nucleosynthesis ashes fall back to the surface of the neutron star due to its deep gravitational potential well, affecting the evolution of its crust. There is a significant bottleneck proceeding from the Hot CNO hydrogen burning cycles to the rp process, which affects energy generation and the observable light curve. The ^{15}O$(α,γ)^{19}$Ne$(p,γ)^{20}$Na reaction sequence is a proposed breakout path to the rp process [4]. The ^{19}Ne$(p,γ)^{20}$Na reaction ($Q = 2190$ keV) [5,6] is expected to be dominated by the only resonance in the Gamow window at 457 keV ($E_x = 2647$ keV) above the proton threshold (Fig. 1) [7]. The matter of its spin and parity has been debated for nearly 30 years because these quantities are crucial to determining the resonance strength. The most likely values for a spin and parity assignment have been suggested to be 1^+ or 3^+ [8]. A $J^π$ of 1^+ would result
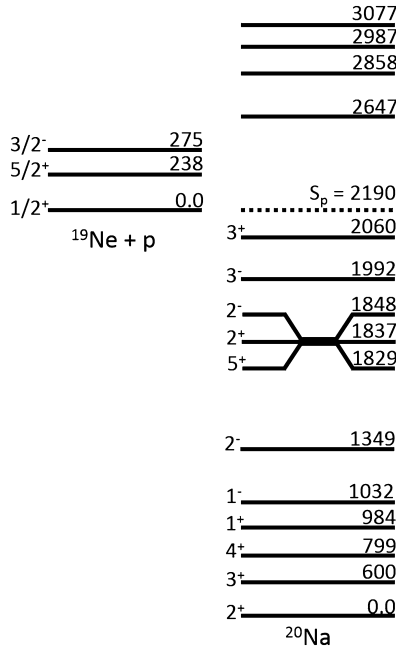
Fig. 1. Relevant low-lying states in ^{19}Ne and ^{20}Na labeled with J^{π} and energy in keV. Energies below the proton threshold in ^{20}Na as well as J^{π} are adopted from Seweryniak et al. [21] and energies above the proton threshold are from Wallace et al. [22].

in a significantly slower reaction rate than a 3^+ assignment [7,9] and would be more likely to cause the ^{19}Ne ($J^{\pi} = 1/2^+$) to return to the hot-CNO cycles rather than breaking out to higher mass nuclei.

Many different types of experiments have been carried out in the past to extract information about the 2647 keV state including stable beam reaction experiments, rare isotope beam experiments and β-decay experiments.

Early experiments focused mainly on stable beam transfer reactions in order to populate the state. Kubono et al. discovered the ~2647 keV ^{20}Na state via the ^{20}Ne(^{3}He,t)^{20}Na [10] reaction and subsequently Lamm et al. remeasured the same reaction and argued for a 1^+ assignment based on a DWBA analysis [11]. Smith et al. also measured the ^{20}Ne(^{3}He,t)^{20}Na reaction and improved the precision of the ^{19}Ne(p,γ)^{20}Na resonance energies [12]. A theoretical study of the mirror energy levels in ^{20}F and ^{20}Na by Brown et al. determined from the available data that a 3^+ assignment of the 2647 keV state was more likely by pairing it with the 2966 keV mirror state in ^{20}F [7]. The state has also been observed via the ^{20}Ne(p,n)^{20}Na reaction through which a 3^+ argument was made based on the angular distribution of the neutrons [13]. Belarge et al. used a rare-isotope beam of ^{19}Ne to measure the ^{19}Ne(d,n)^{20}Na proton transfer reaction and were able to populate the three lowest energy resonances and observe their proton emissions to both the ground state and excited states [14], arguing for a J^{π} of 3^+ for the 2647 keV state based on the analysis of the reconstructed neutron angular distribution.

Rare isotope beams of ^{19}Ne have been used to search for the important resonance directly at astrophysical energies but have only yielded upper limits on the resonance strength of 21 meV [15] and 15 meV [16] with 90% confidence.

The β-decay of ^{20}Mg ($J^{\pi} = 0^+$) to ^{20}Na has been utilized because it constrains the J^{π} of the 2647 keV state experimentally. If the J^{π} of the state were 1^+ then its β-decay feeding by ^{20}Mg would be allowed by β-decay selection rules. However if the state were 3^+ then the β transition would be second-forbidden and very

weak. An early study of ^{20}Mg β-delayed proton decay by Görres et al. determined an upper limit on the feeding of the 2647 keV state to be 2×10^{-3} under the assumption that proton emission dominates over γ-ray emission [17]. Piechaczek et al. also conducted a ^{20}Mg β-decay study which yielded an upper limit on the β-decay feeding of 1×10^{-3} to the 2647 keV state in ^{20}Na [18]. The experiment by Piechaczek et al. searched for protons and also for selected γ-rays but did not find any evidence for the 2647 keV state being populated at their level of sensitivity. A recent study of ^{20}Mg β-delayed proton emission by Wallace et al. yielded the most stringent upper limit on the partial β-decay branch to the 2647 keV state of 2×10^{-4} leading to a partial log ft of >6.9 [9], making a 1^+ assignment unlikely under the implicit assumption that the proton branching ratio is large. Recent experiments by Sun et al. [19] and Lund et al. [20] searched for both protons and γ-rays but did not have enough statistics to improve upon the previous constraints on J^{π}.

Evidently, previous analysis of ^{20}Mg β-decay to the 2647 keV state has relied heavily on the protons emitted from this state and has rarely addressed the γ-ray branch. In fact a complete experimental upper limit on the β-decay feeding of this state has never been set. Either 1^+ or 3^+ assignments should yield a γ-decay branching ratio Γ_{γ}/Γ on the order of 10% [15]. This value is based on theoretical estimates and could be larger. Therefore, it is important to measure the β-delayed γ-decay branch or limit it experimentally. In the present work, we describe a search for these ^{20}Mg β delayed γ-rays to complement the previously measured upper limit [9] on the proton branch.

2. Experiment

The experiment was conducted at the National Superconducting Cyclotron Laboratory (NSCL) [23,24]. A ^{24}Mg primary beam was accelerated using the K500 and K1200 coupled cyclotrons to 170 MeV/u at a nominal current of 60 pnA. The primary beam impinged on a 961 mg/cm^2 ^{9}Be transmission target to produce a fast beam of the desired ^{20}Mg ions in addition to other fragmentation products. The secondary beam was purified using the A1900 magnetic fragment separator [25] and was delivered to the experimental setup.

A 300-μm-thick Si transmission detector was placed $\approx$1 m upstream of the experimental setup. The Si detector was lowered into the beam-line periodically for particle identification measurements using the ΔE-TOF method. The time-of-flight was measured over a 25 m flight path between a scintillator at the focal plane of the A1900 and the Si detector. The beam was implanted into a 26.7-mm-thick plastic scintillator optically coupled to a photomultiplier tube and was used to detect β^+ particles. The scintillator was surrounded by the Segmented Germanium Array (SeGA) in two rings of eight HPGe detectors each in order to detect γ-rays. The signals from each SeGA detector as well as the Si detector and plastic scintillator were processed by the NSCL digital data acquisition system [26].

The beam after the A1900 was composed of 34% ^{20}Mg ($Q_{EC} = 10.7$ MeV), 24% ^{18}Ne ($Q_{EC} = 4.4$ MeV), 12% ^{17}F ($Q_{EC} = 2.8$ MeV), 22% ^{16}O (stable) and 8% ^{15}N (stable) [5]. These beam composition values differ from those reported in Glassman et al. where a 1-D spectrum of the Si detector energy was used to determine the composition [23] whereas analysis of the 2D time of flight vs. Si energy has now enabled a more accurate determination of the composition. These values were only used as a qualitative diagnostic to help identify γ-rays which did not result from ^{20}Mg β-decay.
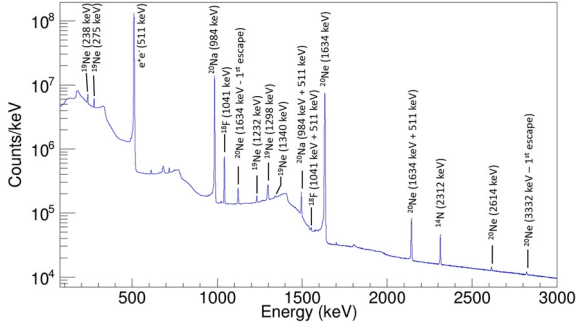
Fig. 2. Cumulative spectrum of ^{20}Mg β-delayed γ-rays acquired by SeGA, in coincidence with β-decay events in the plastic scintillator.

3. Analysis

In order to measure the feeding of the 2647-keV ^{20}Na state, we searched for γ-ray lines in the SeGA spectra corresponding to all possible primary branches by applying exponentially modified gaussian fits of the form

$$f(x; N, \mu, \sigma, \lambda) = B + \frac{N}{2\lambda} \exp\left(\frac{1}{2}\left(\frac{\sigma}{\lambda}\right)^2 - \frac{x-\mu}{\lambda}\right)$$
$$erfc\left(\frac{1}{\sqrt{2}}\left(\frac{\sigma}{\lambda} - \frac{x-\mu}{\sigma}\right)\right) \quad (1)$$

to the spectrum and fixing the mean (μ) over a range of energies. Based on well known unbroadened β-delayed γ lines in the spectrum from ^{20}Na and ^{20}Ne [8] we parameterized the line shape using the width of the Gaussian (σ) and exponential decay constant (λ) as a function of energy and interpolated these values to each region of interest. N is defined to be the area below the curve, B is a linear background, and $erfc$ is the complementary error function.

We determined the intensity of each ^{20}Na γ-ray branch in ^{20}Mg β-decay, using the number of counts in the photopeak N_E at γ-ray energy E, the photopeak efficiency of SeGA at energy E, $\mathcal{E}_E$, and the number of ^{20}Mg ions implanted into the plastic scintillator, $N_{20_{Mg}}$, as input to the following equation:

$$I_{\beta\gamma}^E = \frac{N_E}{\mathcal{E}_E N_{20_{Mg}}} \quad (2)$$

A first order γ-ray energy calibration of the SeGA detectors was applied to the pulse height spectra in each run by performing a gain matching using strong room-background lines from the β-decays of ^{40}K and ^{208}Tl which produced γ-ray energies of 1460.851 ± 0.006 keV [27] and 2614.511 ± 0.010 keV [28], respectively. Peaks were fit using an exponentially modified gaussian function (Eq. (1)) added to a local background model (usually a linear function) to determine the centroids. A cumulative spectrum incorporating all 16 SeGA detectors was generated by applying a coincidence gate in the timing spectrum between SeGA and scintillator events in order to select the γ-rays originating from a β-decay event (Fig. 2). By applying this timing gate we were able to compare the ratio of photopeak counts in the ungated spectrum to the counts in the gated spectrum. This yielded a consistent ungated to gated ratio of 0.90(1) for ^{20}Na and ^{20}Ne peaks over a broad energy range representing the constant efficiency of the scintillator to detect β particles from ^{20}Mg β-decay. Further energy calibration was applied to the cumulative spectrum [23] to account for second order effects, which affected the calibration by less than 1 keV.
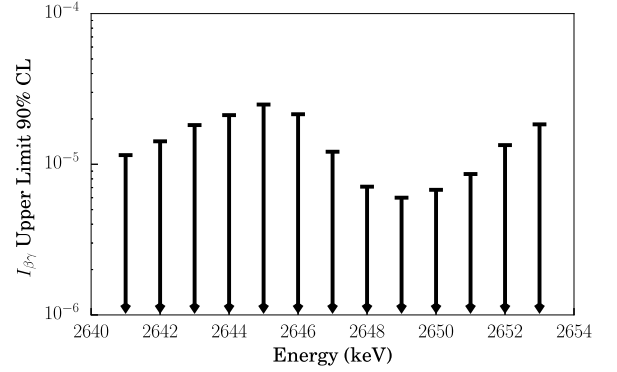

Fig. 3. Measured 90% C.L. upper limits on the intensity of ^{20}Mg β delayed γ-rays as a function of energy in the 2647 keV search region. The most conservative limit is at 2645 keV.
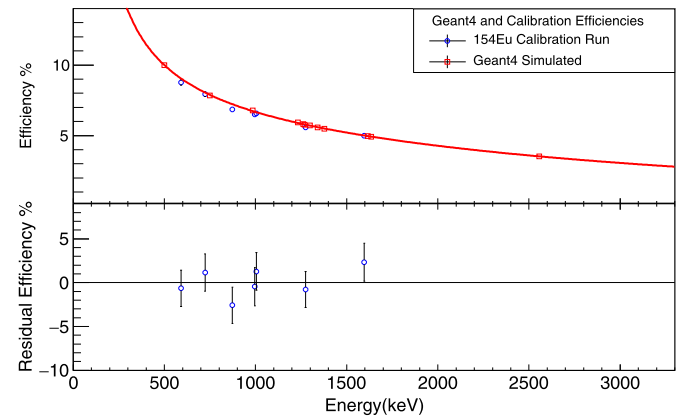

Fig. 4. Upper panel: Photopeak efficiency of SeGA as a function of energy. Circles correspond to efficiencies from the Eu calibration source. Squares correspond to efficiencies from a GEANT4 simulation of the experimental setup. Fit function (3) was used to model the GEANT4 simulation efficiency. The fit was then scaled by a constant factor to line up with the source calibration efficiency (red line). Lower panel: The residual efficiency is the relative difference between the calibration source data and the scaled fit of GEANT4 simulation efficiencies. (For interpretation of the references to color in this figure legend, the reader is referred to the web version of this article.)

The photopeak γ-ray detection efficiency of SeGA, up to 1596 keV, was measured using an absolutely calibrated ^{154}Eu source placed in the center of the front face of the plastic scintillator (Fig. 4). The total number of ^{20}Mg ions implanted into the scintillator ($N_{20_{Mg}}$) was calculated indirectly using the number of counts in the 984 keV transition peak, the known ^{20}Mg β-delayed γ-decay intensity of the 984 keV transition in ^{20}Na of 0.697 ± 0.012 [18] (recently confirmed in [20]) and the efficiency at this energy, which was determined to be $\mathcal{E}_{984} = 0.0653 \pm 0.0025$ by interpolating the efficiency data from the calibration source.

A GEANT4 Monte Carlo simulation was used to model the experimental setup and simulate an independent efficiency curve. In order to match our experimental conditions, monoenergetic γ-rays were emitted isotropically from the center of the scintillator and interacted with the surrounding SeGA array to produce a gamma ray spectrum. The photopeak efficiency was extracted from the generated spectrum and this procedure was repeated over a wide range of energies from 0 to 8 MeV for comparison with the experimental data. Comparison of GEANT4 simulations of γ-rays emitted from the center of the scintillator versus the front face of the scintillator showed a negligible difference in total photopeak efficiency due to the $\approx$1 cm difference in calibration source position and
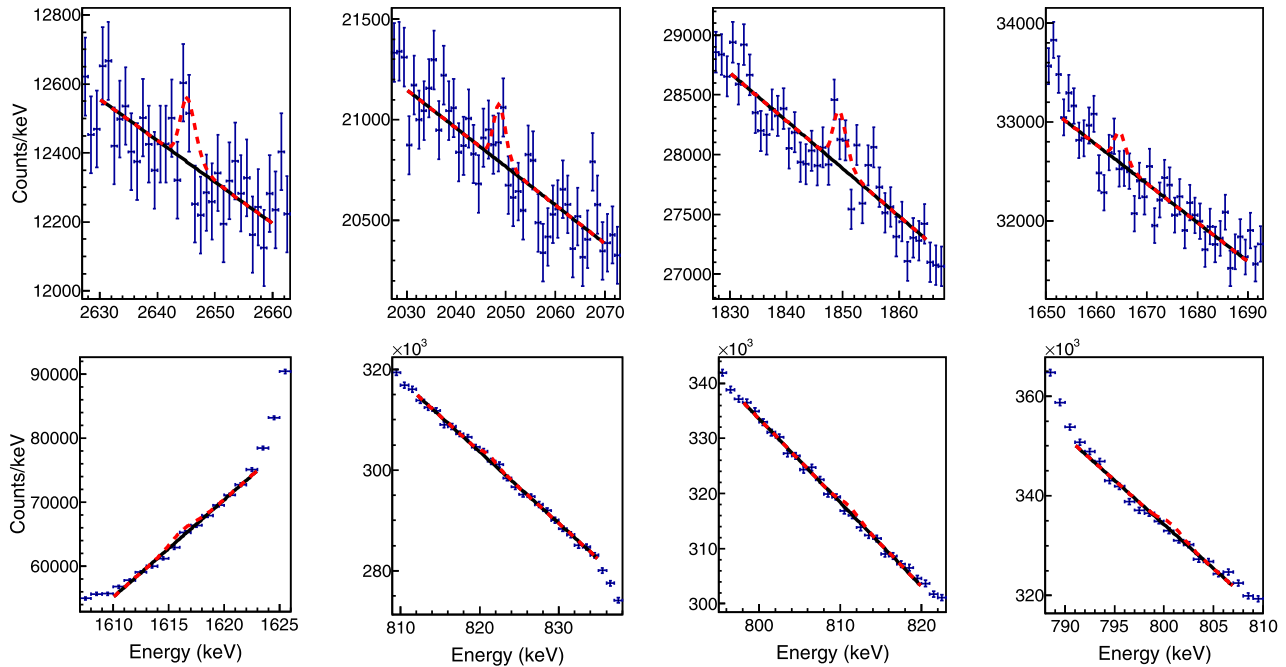
Fig. 5. Each panel shows a magnified region of the spectrum of ^{20}Mg β-delayed γ-rays acquired by SeGA, in coincidence with β-decay events in the plastic scintillator (Fig. 2). The regions of interest are determined by the possible transition energies from the 2647-keV state in ^{20}Na (Table 1). The blue points represent the data with statistical error bars and the black lines a linear fit of the background. The red dotted lines represent the background fit plus the 90% confidence upper limits for each possible transition energy. For each transition the fit shown corresponds to the energy within the ±6 keV search range that yielded the maximum upper limit. (For interpretation of the references to color in this figure legend, the reader is referred to the web version of this article.)

online source position, allowing us to treat our calibration source data without any correction for source position.

The discrete GEANT4 efficiency curve was interpolated with a continuous function of form (Eq. (3))

$$\ln(\mathcal{E}) = \sum_{i=0}^{i=5} C_i (\ln(E))^i \qquad (3)$$

and compared to the calibration data (Fig. 4). The ratio of the GEANT4 simulation efficiencies to the efficiencies from calibration data show that we can scale the GEANT4 simulation by a constant normalization factor of 0.975 to fall in line with the data. We therefore used the scaled functional form representing the GEANT4 simulation to interpolate and extrapolate the efficiency continuously as a function of energy. The systematic uncertainty associated with extrapolating was estimated to be ≤5% for γ-ray energies <2.7 MeV. Statistical uncertainties associated with the calibration data were obtained from the exponentially modified gaussian fits. Systematic uncertainties associated with the source were calculated from uncertainties in the branching ratios and were determined to be ≤1%. A simulation was done in GEANT4 to account for the loss of photopeak counts due to $\gamma-\gamma$ summing effects which resulted in a 2% systematic uncertainty at all energies. All uncertainties were combined in quadrature to determine a total efficiency uncertainty for each γ-ray line from the source.

4. Results and discussion

No significant γ-ray peaks were observed to correspond with the eleven possible transition energies deexciting the 2647-keV state of ^{20}Na. The upper limit on $I_{\beta\gamma}$ for all but three branches was determined by a single exponentially modified Gaussian (Eq. (1)) with linear background fit over a range of energies (Fig. 5). For two of the other three branches a Gaussian + linear function was used to represent the background (Fig. 6) because of a narrow

Table 1
Upper limits on the intensities of ^{20}Mg β-delayed γ-ray transitions through the 2647-keV ^{20}Na state with 90% confidence. Final energy level values were adopted from Seweryniak et al. [21]. The search for each γ-ray encompassed a range of ± 6 keV.

^{20}Na γ-ray Transition (keV)	Transition Energy (keV)	$I_{\beta\gamma}$
2647 → 0	2647	< 2.5 × 10^{-5}
2647 → 600	2047	< 3.7 × 10^{-5}
2647 → 799	1848	< 5.5 × 10^{-5}
2647 → 984	1663	< 3.5 × 10^{-5}
2647 → 1032	1615	< 1.0 × 10^{-4}
2647 → 1349	1298	< 5.3 × 10^{-4}
2647 → 1829	818	< 5.6 × 10^{-5}
2647 → 1837	810	< 6.7 × 10^{-5}
2647 → 1848	799	< 8.9 × 10^{-5}
2647 → 1992	655	< 2.7 × 10^{-5}
2647 → 2060	587	< 8.2 × 10^{-5}

background peak near the search region. Searching for the peak at 1298 keV was complicated by the fact that it lies at nearly the same energy as a Doppler-broadened ^{19}Ne peak [29]. In this special case a Monte Carlo method was used to fit the Doppler-broadened ^{19}Ne peak using known proton intensities and energies [18,20]. In the simulation, protons were emitted isotropically from the center of the plastic scintillator and the stopping power was determined by SRIM. The relative proton intensities and energies were fixed, which determined the peak shape, and the overall normalization was left as a free parameter. Due to incomplete charge collection associated with the large peak, we couldn't model the continuum with a simple linear function. Instead we connected two linear functions (to represent the distinct backgrounds on either side of the peak) using a continuous step underneath the Doppler-broadened peak. The Doppler-broadened peak was added to this function and used to model the total background. A narrow ^{20}Na peak was searched for on top of the background (Fig. 7).
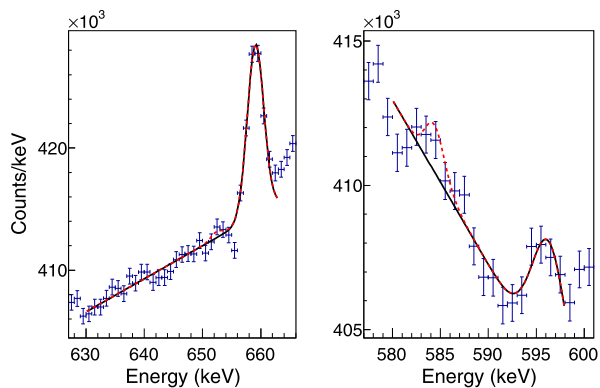
Fig. 6. Each panel shows a magnified region of the spectrum of ^{20}Mg β-delayed γ-rays acquired by SeGA, in coincidence with β-decay events in the plastic scintillator (Fig. 2). The regions of interest are determined by the possible transition energies from the 2647-keV state in ^{20}Na (Table 1). The blue points represent the data with statistical error bars and the black lines a linear plus Gaussian fit for the background. The red dotted lines represent the background fit plus the 90% confidence upper limits for each possible transition energy. For each transition the fit shown corresponds to the energy within the ± 6 keV search range that yielded the maximum upper limit. (For interpretation of the references to color in this figure legend, the reader is referred to the web version of this article.)
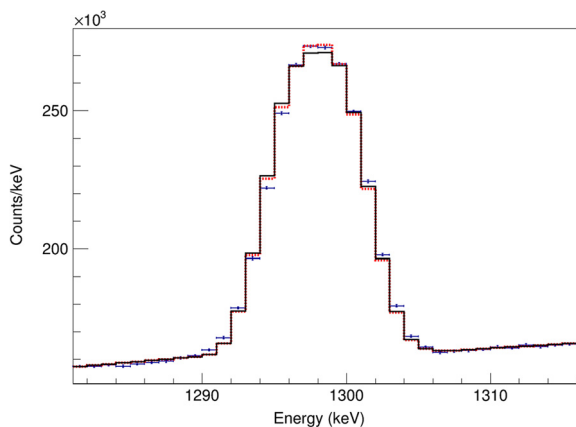

Fig. 7. A magnified region of the spectrum of ^{20}Mg β-delayed γ-rays acquired by SeGA, in coincidence with β-decay events in the plastic scintillator (Fig. 2). The blue points represent the data with statistical error bars. The black line represents the background Monte Carlo plus continuum background model described in the text. The red dotted line represents the background Monte Carlo fit plus the 90% confidence upper limits for the 1298 keV transition energy. The fit shown corresponds to the energy within the ± 6 keV search range that yielded the maximum upper limit. (For interpretation of the references to color in this figure legend, the reader is referred to the web version of this article.)

Each individual transition was searched for over a ± 6 keV range about its nominal value to cover any potential inaccuracies in the literature energy of the 2647-keV state. The fitting procedure output the number of counts in the peak and a corresponding uncertainty represented together by a Gaussian probability density function (PDF). The 90% C.L. upper limit on the number of counts was determined by integrating the PDF from zero to 90% of the integral from zero to infinity. By applying Equation (2), the most conservative upper limit on the intensity in the search range was determined for each transition (Table 1). For example, Fig. 3 shows the intensity upper limits in the search range for the 2647-keV γ-ray.

To find the total upper limit on $I_{\beta\gamma}$, the intensity for each transition was calculated from the central value of the number of counts using Equation (2). The intensities were summed and the uncertainties were added in quadrature to produce a Gaussian PDF representing $I_{\beta\gamma}$. The 90% C.L. upper limit on $I_{\beta\gamma}$ was determined
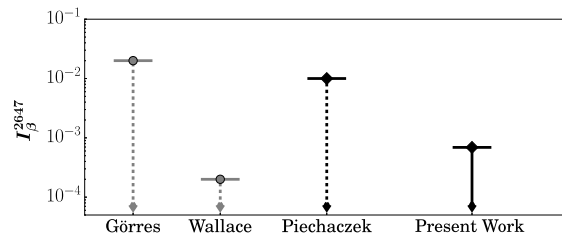

Fig. 8. Upper limits on the intensity of the ^{20}Mg β-decay transition to the 2647 keV state of ^{20}Na compiled from different sources [17,18,9]. All of the upper limits from previous work (dashed lines) are incomplete. The upper limits in grey include only the proton branch to the ground state of ^{19}Ne. The upper limit by Piechaczek includes the proton branch to the ground state and selected γ-ray branches. The present work includes proton branches to the g.s. and 1st excited state in ^{19}Ne [9, 14] as well as all energetically possible γ branches in ^{20}Na, making it the only complete limit.

Table 2
Gamow–Teller strengths B(GT) and associated log ft values calculated for ^{20}Mg β-decay to 1st and 2nd excited 1^+ states in ^{20}Na using the sd shell model with various interactions described in the text.

Interaction	B(GT) 1^+_1	log ft 1^+_1	B(GT) 1^+_2	log ft 1^+_2
USD	0.366	4.03	0.994	3.59
USDA	0.431	3.96	0.494	3.89
USDB	0.460	3.93	0.621	3.80
USDB-EDF	0.446	3.94	0.587	3.82
IMSRG	0.828	3.67	0.377	4.01

by integrating the PDF from zero to 90% of the integral from zero to infinity. In this procedure, a single value of the excitation energy of the 2647-keV state was used for all transitions. By repeating this procedure over the ± 6 keV search range, the maximum value of the upper limit was found to be $I_{\beta\gamma} < 5.7 \times 10^{-4}$.

Wallace et al. determined the proton intensity from the 2647 keV state to be $I_{\beta p} < 2 \times 10^{-4}$ [9]. However, this limit did not include the recently detected proton emission to the 1st excited state of ^{19}Ne at 238 keV, which Belarge et al. measured to have approximately the same branching ratio as emission to the ground state [14]. The inclusion of this new path leads to $I_{\beta p} < 4 \times 10^{-4}$. The underlying PDF representing $I_{\beta p}$ was not documented in Wallace et al. so we assume that their uncertainties were also dominated by statistics and that they followed a procedure similar to ours. Adding their limit on $I_{\beta p}$ with our limit on $I_{\beta\gamma}$ in quadrature yields the first complete experimental limit of $I_\beta < 6.9 \times 10^{-4}$ and log $ft > 6.4$ for the ^{20}Mg β^+ decay transition to the 2647-keV ^{20}Na state (see Fig. 8).

For comparison to the experimental limit, we calculated theoretical values of log ft for the transition to the unbound 2nd 1^+ state of interest as well as the bound 984 keV 1^+ state utilizing the sd shell model with harmonic oscillator radial wave functions and a quenching of 0.6 (Table 2). In order to assess the uncertainty in this calculation, a variety of interactions were used including USD [31], USDA [32], USDB [32], USDB-EDF, and IMSRG [33–35]. The USDB-EDF calculation was used to assess the uncertainties associated with the radial wave functions for the loosely-bound states involved and the EDF part was obtained with the Skx Skyrme functional [36]. All calculated log ft values for the bound 984 keV state were in the range 3.67–4.03. This agrees with the measured values of 3.87 [30] and 3.83 $\pm$ 0.02 [18]. Similarly, the range of values we expect for the transition to the 2nd excited 1^+ state in ^{20}Na is 3.59–4.01, much lower than the measured log $ft > 6.4$. Therefore, the 2647-keV state does not correspond to the 1^+ state from the shell model. In fact, the 2647 keV state is likely not any 1^+ state because configuration mixing should result in smaller log ft values than observed even for an intruder 1^+ state.

Considering a 3^+ assignment, the log ft values of second forbidden $\Delta J = 3$ β-decay transitions in the mass region $9 < A < 27$ are all greater than 14 [37]. Our limit of $\log ft > 6.4$ for the transition from $J^\pi = 0^+$ ^{20}Mg to the 2647 keV state is, therefore, consistent with a 3^+ assignment; however, this does not exclude other possibilities for the J^π assignment.

The 2987 keV ^{20}Na state is most likely the analog of the 1^+ ^{20}F state at 3488 keV [7,22]. log ft values of 4.08(6) and 4.07(3) were measured in the previous work for the feeding of this ^{20}Na state [18,20], which is essentially consistent with the range 3.59–4.01 predicted by our shell model calculations for the 2nd 1^+ state.

5. Conclusion

An intense source of ^{20}Mg and a γ-ray spectrometer with high resolution and efficiency were used to search for population of the 2647 keV state in ^{20}Na via β-decay. For the first time, all possible γ-ray branches from this state were limited in order to complement previous searches for the proton branch. An upper limit on the β delayed γ decay intensity was measured completing the limit on the log ft value. The combined results from the present ^{20}Mg($\beta\gamma$) experiment and past ^{20}Mg(βp) [9] and ^{19}Ne(d,n)^{20}Na experiments [14] make an assignment of 1^+ highly unlikely, in agreement with recent work.

Acknowledgements

References

[1] H. Schatz, K.E. Rehm, Nucl. Phys. A 777 (2006) 601.
[2] W.H.G. Lewin, J.V. Paradijs, R.E. Taam, Space Sci. Rev. 62 (1993) 223.
[3] R.K. Wallace, S.E. Woosley, Astrophys. J. Suppl. Ser. 45 (1981) 389.
[4] H. Schatz, et al., Phys. Rev. Lett. 86 (2001) 3471.
[5] G. Audi, et al., Chin. Phys. C 41 (2017) 030001.
[6] C. Wrede, et al., Phys. Rev. C 81 (2010) 055503.
[7] B.A. Brown, A.E. Champagne, H.T. Fortune, R. Sherr, Phys. Rev. C 48 (1993) 1456.
[8] D.R. Tilley, C.M. Cheves, J.H. Kelley, S. Raman, H.R. Weller, Nucl. Phys. A 636 (1998) 249.
[9] J.P. Wallace, et al., Phys. Lett. B 712 (2012) 59.
[10] S. Kubono, et al., Z. Phys. A 331 (1988) 359.
[11] L.O. Lamm, et al., Nucl. Phys. A 510 (1990) 503.
[12] M.S. Smith, et al., Nucl. Phys. A 536 (1992) 333.
[13] B.D. Anderson, et al., Phys. Rev. C 52 (1995) 2210.
[14] J. Belarge, et al., Phys. Rev. Lett. 117 (2016) 182701.
[15] G. Vancraeynest, et al., Phys. Rev. C 57 (1998) 2711.
[16] M. Couder, et al., Phys. Rev. C 69 (2004), 022801(R).
[17] J. Görres, et al., Phys. Rev. C 46 (1992) R833.
[18] A. Piechaczek, et al., Nucl. Phys. A 584 (1995) 509.
[19] L.J. Sun, et al., Phys. Rev. C 95 (2017) 014314.
[20] M.V. Lund, et al., Eur. Phys. J. A 52 (2016) 304.
[21] D. Seweryniak, et al., Phys. Lett. B 590 (2004) 170.
[22] J.P. Wallace, P.J. Woods, Phys. Rev. C 86 (2012) 068801.
[23] B.E. Glassman, et al., Phys. Rev. C 92 (2015), 042501(R).
[24] C. Wrede, et al., Phys. Rev. C 96 (2017), 032801(R).
[25] D.J. Morrissey, et al., Nucl. Instrum. Methods Phys. Res., Sect. B 204 (2003) 90.
[26] C.J. Prokop, et al., Nucl. Instrum. Methods Phys. Res., Sect. A 741 (2014) 163.
[27] J. Chen, Nucl. Data Sheets 140 (2017) 1.
[28] M.J. Martin, Nucl. Data Sheets 108 (2007) 1583.
[29] S.B. Schwartz, et al., Phys. Rev. C 92 (2015), 031302(R).
[30] S. Kubono, et al., Phys. Rev. C 46 (1992) 361.
[31] H.T. Fortune, B.H. Wildenthal, Phys. Rev. C 30 (1984) 1063.

[32] W.A. Richter, S. Mkhize, B. Alex Brown, Phys. Rev. C 78 (2008) 064302.
[33] S.R. Stroberg, H. Hergert, J.D. Holt, S.K. Bogner, A. Schwenk, Phys. Rev. C 93 (2016) 051301.
[34] J. Simonis, et al., Phys. Rev. C 98 (2017) 014303.
[35] S.R. Stroberg, private communication.
[36] B.A. Brown, Phys. Rev. C 58 (1998) 220.
[37] E.K. Warburton, Phys. Rev. C 45 (1992) 463.